Miao et al. *Zool. Res.* 2024, 45(5): 1161−1174
https://doi.org/10.24272/j.issn.2095-8137.2024.072
https://cstr.cn/32248.14.zr.2024.072

ZR | Zoological Research

Review Open Access

Experimental models for preclinical research in kidney disease

Jin Miao[1,#], Huanhuan Zhu[1,#], Junni Wang[1], Jianghua Chen[1], Fei Han[1,*], Weiqiang Lin[2,*]

[1] *Kidney Disease Center*, *First Affiliated Hospital*, *Zhejiang University School of Medicine*; *Institute of Nephrology*, *Zhejiang University*; *Key Laboratory of Kidney Disease Prevention and Control Technology*, *Zhejiang Province*; *Zhejiang Clinical Research Center of Kidney and Urinary System Disease*, *Hangzhou*, *Zhejiang* 310003, *China*

[2] *Department of Nephrology*, *Center for Regeneration and Aging Medicine*, *Fourth Affiliated Hospital of School of Medicine*, *and International School of Medicine*, *International Institutes of Medicine*, *Zhejiang University*, *Yiwu*, *Zhejiang* 322000, *China*

ABSTRACT

Acute kidney injury (AKI) and chronic kidney disease (CKD) are significant public health issues associated with a long-term increase in mortality risk, resulting from various etiologies including renal ischemia, sepsis, drug toxicity, and diabetes mellitus. Numerous preclinical models have been developed to deepen our understanding of the pathophysiological mechanisms and therapeutic approaches for kidney diseases. Among these, rodent models have proven to be powerful tools in the discovery of novel therapeutics, while the development of kidney organoids has emerged as a promising advancement in the field. This review provides a comprehensive analysis of the construction methodologies, underlying biological mechanisms, and recent therapeutic developments across different AKI and CKD models. Additionally, this review summarizes the advantages, limitations, and challenges inherent in these preclinical models, thereby contributing robust evidence to support the development of effective therapeutic strategies.

Keywords: Acute kidney injury; Chronic kidney disease; Mouse models

INTRODUCTION

Acute kidney injury (AKI) is a clinical syndrome characterized by a marked reduction in glomerular filtration rate (GFR), leading to the accumulation of nitrogenous waste products such as creatinine and urea nitrogen, along with disturbances in fluid, electrolyte, and acid-base homeostasis. The current diagnostic criteria for AKI include one or more of the following: (1) an increase in serum creatinine (SCr) greater than 0.3 mg/dL (26.5 μmol/L) within 48 hours; (2) an increase in SCr of more than 50% from the basal value within 7 days; and (3) a reduction in urinary output to less than 0.5 mL/kg/h for a duration exceeding 6 hours (Kellum et al., 2021). AKI is increasingly recognized as a major public health concern, affecting millions worldwide and significantly reducing survival rates. AKI also serves as a risk factor for the initiation and progression of chronic kidney disease (CKD), which can culminate in end-stage renal disease (Singbartl & Kellum, 2012; Zhang et al., 2022). CKD itself is a significant global health challenge, diagnosed by either the presence of albuminuria or a reduction in estimated GFR (eGFR) to less than 60 mL/min/1.73 m² (Andrassy, 2013). CKD is associated with elevated morbidity and mortality rates, primarily due to cardiovascular complications. Early detection and treatment of CKD risk factors are essential for its prevention. Despite significant advances in experimental models of AKI and CKD that replicate the complex pathophysiology of human kidney diseases (Fu et al., 2018), notable gaps remain in our understanding, requiring further investigation.

Rodent models, particularly murine models, have been extensively utilized in kidney disease research. Recent advancements in technology have led to the continuous refinement of these models, resulting in the development of increasingly sophisticated and accurate representations of kidney disease. This review critically examines the latest advancements in AKI and CKD model systems, offering a comprehensive analysis of their benefits, limitations, and inherent challenges in translating findings into clinical applications.

ACUTE KIDNEY INJURY

Various AKI models have been developed to investigate the underlying pathogenesis and to evaluate potential therapeutic interventions (Figure 1). The most widely utilized models

Received: 03 March 2024; Accepted: 04 June 2024; Online: 05 June 2024

Foundation items: This work was supported by the Zhejiang Provincial Natural Science Foundation of China (LZ22H050001), National Natural Science Foundation of China (82270704, 81970573), “Lingyan” R&D Research and Development Project (2024C03165), and Zhejiang Provincial Program for the Cultivation of High-level Innovative Health Talents

[#]Authors contributed equally to this work

*Corresponding authors, E-mail: hanf8876@zju.edu.cn; wlin@zju.edu.cn

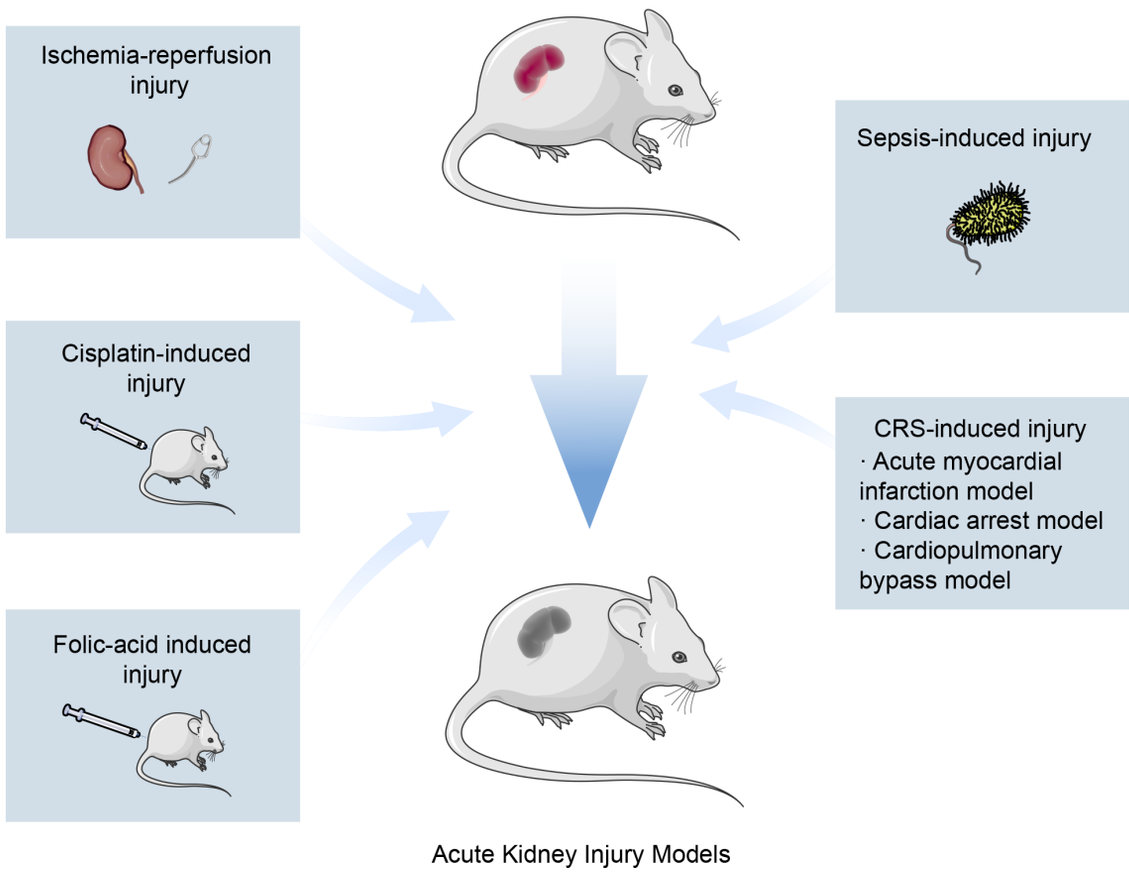

Figure 1 Rodent models of acute kidney injury (AKI)

Precisely defined experimental models of AKI offer considerable potential for recapitulating the diverse pathophysiology of human AKI. IR models are typically generated by surgical clamping of the renal artery. AKI can also be induced in mice by administering agents such as cisplatin, folic acid, or lipopolysaccharide (LPS). AKI models related to cardiorenal syndrome (CRS) can also be induced through different types of heart surgeries performed on mice.

include those induced by ischemia-reperfusion (IR), cisplatin, and sepsis, with less frequently employed models including those induced by diverse nephrotoxic drugs. In recent years, human kidney organoids—three-dimensional (3D) structures generated from pluripotent stem cells *in vitro*—have emerged as a novel and promising model for studying AKI, offering unique insights into disease mechanisms and therapeutic responses that were previously unattainable.

Ischemia-reperfusion models

In rodent models, especially mice, renal IR injury is commonly induced through surgical clamping of the renal pedicles. Prior to the procedure, anesthetics and sterile surgical instruments are prepared and a heating pad is pre-warmed to maintain a surgical temperature between 35°C and 37°C. The procedure begins with the intraperitoneal administration of pentobarbital sodium to anesthetize the mouse A small vertical flank incision or abdominal median incision, approximately 1.5 cm in length, is then made to access the renal hilum. A non-traumatic arterial clip is gently clamped to the renal pedicle to induce ischemia for a predetermined duration. In previous research, we established reproducible IR conditions by applying IR at 35°C for 30 minutes and at 37°C for 25 minutes. Successful induction of ischemia is confirmed by the uniform darkening of the kidney during the ischemic phase (Cheng et al., 2022).

AKI becomes evident within 24 hours post-surgery, characterized by significant elevations in SCr and blood urea nitrogen (BUN). Histological examination of PAS-stained renal cortex sections shows renal injuries, including loss of the brush border, vacuolization in tubular cells, and formation of casts (Hosohata et al., 2021). Further assessment of renal damage, such as tubular dilatation, tubular necrosis, and inflammatory responses, can be quantified through semi-quantitative grading of hematoxylin-eosin (H&E)-stained kidney samples (Chu et al., 2022). Moreover, significant increases in kidney injury molecule-1 (KIM-1), neutrophil gelatinase-associated lipocalin (NGAL), interleukin-6, and tissue inhibitor of metalloproteinase-2 have been observed after IR injury (Cheng et al., 2022; Shiva et al., 2020; Wang et al., 2024).

In mice, AKI can be induced through bilateral or unilateral IR injury. Bilateral clamping of the renal arteries is often employed to simulate AKI, as it significantly reduces renal mass and function, leading to elevated SCr and BUN within 24 hours, hallmarks of clinical AKI (Shiva et al., 2020). However, the use of prolonged clamping times in bilateral IR models is constrained due to the high mortality rates associated with extensive renal ischemia. To address the limitations of bilateral IR, unilateral IR models with immediate contralateral nephrectomy are often employed, which permit extended ischemia durations and facilitate the study of AKI after a long post-IR phase (Lech et al., 2009). Furthermore, unilateral IR with preservation of the contralateral kidney greatly reduces mortality risk from renal failure, thereby providing a more stable platform for evaluating AKI progression and outcomes (Shiva et al., 2020).

Operational challenges are inevitable during IR procedures. One frequent issue is incomplete renal ischemia. To mitigate this, it is recommended to use consistently branded clamps, periodically renew vascular clamps (Cheng et al., 2022), minimize the inclusion of fatty tissue during renal artery isolation, and, if necessary, deploy two vascular clamps to ensure complete ischemia. Bleeding complications are another significant concern during surgery, including mesenteric arterial bleeding, renal parenchymal bleeding, and renal arterial bleeding. A thorough understanding of the mouse abdominal anatomy and careful handling during surgery are essential for minimizing these risks. Minor bleeding can typically be controlled with gauze or cotton swabs; however, if blood loss exceeds 0.4 mL, it may result in hemorrhagic shock-induced AKI, necessitating exclusion from the study (Cheng et al., 2022).

Several key factors influence the response to IR injury, including genetic factors, age, sex, type of vascular clamps, anesthetic agents, body weight, and heating systems used during surgery (Kher et al., 2005; Rudman-Melnick et al., 2020). Among these, surgical temperature and ischemia duration are the two most critical determinants of IR injury outcomes. Hypothermia is protective against kidney injury (Abou Taka et al., 2022), whereas excessively high temperatures can cause intraoperative death. Too short ischemia duration may not induce sufficient tubular necrosis to meet AKI criteria, while prolonged ischemia can result in acute tubular necrosis, renal failure, and rapid death (Shiva et al., 2020). In our research, an optimal surgical temperature of 37°C and an ischemic duration of 20–30 minutes have been found to be appropriate (Wang et al., 2021). Additionally, the choice of mouse strain is critical, as different strains exhibit varying sensitivity to IR injury. For example, C57BL/6 mice are more susceptible to IR-induced damage compared to 129/Sv mice (Shiva et al., 2020). Therefore, careful selection of experimental animal species is required before initiating the study.

Cisplatin-induced models

Cisplatin, a widely used in chemotherapeutic agent for solid tumors, is also associated with well-known nephrotoxic complications. Two principal approaches are employed to develop cisplatin-induced AKI models: short-term high-dose and long-term low-dose (Holditch et al., 2019). The short-term high-dose model is generated by administering a single intraperitoneal injection of high-dose cisplatin (approximately 20–30 mg/kg). Injury typically peaks within 48–72 hours post-injection, with significant tubular damage, inflammation, oxidative stress, mitochondrial dysfunction, and cell death evident in the kidneys (Hukriede et al., 2022). However, the severity of the damage often leads to high mortality within a few days, limiting the feasibility of long-term studies. Conversely, the long-term low-dose model involves the administration of a relatively low dose of cisplatin (5–15 mg/kg) over a period of 2 to 4 weeks (Sharp et al., 2018). While this model may not exhibit significant changes in BUN levels, urinary biomarkers such as NGAL typically increase within 1–3 days of cisplatin application. The model also induces a substantial decline in GFR, along with persistent renal fibrosis and peritubular capillary thinning that can last for several months (Hukriede et al., 2022).

Despite the advancements provided by the aforementioned models in expanding our understanding of AKI pathophysiology, they still fall short in replicating the complexities observed in clinical settings, particularly in cancer patients undergoing cisplatin treatment. To bridge this gap, researchers have developed several allograft models, where the AKI model mice also bear tumors. These models use a variety of murine-derived cell lines, including EL4 lymphoblastic cells (Baghdadi et al., 2012), CMT167 pulmonary adenocarcinoma cells (Ravichandran et al., 2018; Ravichandran et al., 2016), H22 hepatocellular carcinoma cells (Li et al., 2015), and CT26/WT fibroblast colon carcinoma cells (Kumar et al., 2017). Following tumor establishment, mice are administered a single dose of cisplatin (20–25 mg/kg) with or without nephroprotective interventions (Holditch et al., 2019). Several weeks post-cisplatin administration, significant increases in BUN, SCr, and NGAL are observed (Ravichandran et al., 2018). These allograft models also present additional complexities that may exacerbate AKI, including tumor lysis syndrome, tumor infiltration of renal tissue, and thrombotic microangiopathy. However, a detailed characterization of renal injury in these models remains lacking. Currently, these models are primarily used to assess the chemotherapeutic efficacy of secondary treatments and their protective effects on renal function. However, further studies are needed to better characterize these tumor-bearing models compared to tumor-free models.

Proximal tubule-localized transporters, including multidrug and toxin extrusion transporter 1 and organic cation transporter 2, play a crucial role in the renal uptake and excretion of cisplatin. This transport process is closely associated with increased oxidative stress, impaired mitochondrial function, and altered expression of endogenous antioxidant enzymes. Proximal tubular epithelial cells (PTECs) are the main target of cisplatin-induced toxicity (Ozkok & Edelstein, 2014). Recently, ferroptosis, a form of regulated cell death, has garnered significant attention in the context of cisplatin-induced AKI. Various studies have demonstrated the therapeutic potential of ferroptosis inhibition in protecting renal function through agents such as vitamin D receptor agonists (Hu et al., 2020), polydatin (Zhou et al., 2022), and dihydromyricetin (Xu et al., 2023). Although the regulatory role of ferroptosis in AKI has been investigated, the precise mechanisms governing this process remain incompletely understood. Recent research has identified the farnesoid X receptor (FXR) as a key regulator of lipid peroxidation and ferroptosis, exerting protective effects against cisplatin-induced AKI by regulating the transcription of genes associated with ferroptosis (Kim et al., 2022). Furthermore, the Ras homolog enriched in the brain has been shown to alleviate cisplatin-induced AKI by preserving mitochondrial homeostasis (Lu et al., 2020), while polydatin has been found to attenuate ferroptosis in cisplatin-induced AKI by modulating the systemic Xc-pathway and inhibiting iron metabolism disorders (Zhou et al., 2022). These findings open new avenues for research into the mechanisms and potential therapeutic targets in cisplatin-induced mouse models of AKI.

Folic acid (FA)-induced models

Folic acid, essential for protein synthesis, cell division, and normal red blood cell production, has been used to create rodent models of AKI. To induce AKI, a high dose of folic acid —typically administered as a single intraperitoneal injection at 250 mg/kg—can precipitate the condition within 72 hours, characterized with proteinuria and elevated BUN and

SCr (Yan, 2021). FA-induced AKI models can replicate the clinical symptoms observed in human AKI, with a high level of reproducibility. To date however, specific biomarkers for FA-induced AKI have not yet been identified. An additional advantage of this model is its kidney-specific toxicity, with few adverse effects on other organs (Yan, 2021).

Studies have confirmed that FA-induced renal injury predominantly affects the proximal renal tubules (Aparicio-Trejo et al., 2020; Li et al., 2021). FA rapidly crystallizes within the renal tubules, triggering a cascade of pathological events including acute tubular necrosis, renal cortical scarring, and epithelial regeneration. This progression ultimately results in kidney injury, characterized by reduced GFR, inflammation, and fibrosis. While the underlying mechanisms involve oxidative stress, ferroptosis, and compromised mitochondrial function, the precise molecular and biochemical pathways driving FA-induced AKI remain to be clarified (Yan, 2021).

Sepsis-induced models

Sepsis-associated AKI (SA-AKI) is a significant contributor to high morbidity and mortality (Peerapornratana et al., 2019), although its pathophysiological mechanisms are complex and incompletely understood. Two primary models are used to investigate SA-AKI: (1) single intraperitoneal injection of lipopolysaccharide (LPS) at a dose of 10–15 mg/kg; and (2) cecal ligation and puncture (CLP) operation.

The LPS-induced model triggers sterile inflammation, leading to a significant increase in SCr and BUN levels within 24 hours post-injection. Researchers consider the AKI model successful when SCr levels increase to at least twice the baseline compared to control littermates (Ren et al., 2020). However, the model presents a challenge due to the narrow therapeutic window between the dose required to induce AKI and the dose that proves lethal.

The CLP model, which better replicates the complex pathophysiology of clinical sepsis, typically induces more severe and prolonged AKI compared to the LPS model. The procedure involves ligating the cecum distal to the ileocecal valve, followed by two needle punctures to allow fecal contents to escape the intestinal lumen. The size of the needle and the number of punctures can significantly influence model severity. This process results in the sustained release of fecal contents, leading to a progressive increase in bacterial load and subsequent sepsis. In this model, organ failure is observed at varying times, with hepatic failure generally preceding renal failure (Hukriede et al., 2022). Due to the down-regulation of creatinine production in sepsis, SCr is not a reliable marker for kidney injury in this model. However, a decline in eGFR is typically observed a few hours after surgery (Street et al., 2018). Although renal histological damage is relatively mild in this model, vacuole-like structures are evident in PTECs (Hukriede et al., 2022).

Three fundamental mechanisms underlying sepsis-induced injury include inflammation, microcirculatory dysfunction, and metabolic reprogramming (Peerapornratana et al., 2019). Inflammation, a previously undervalued component of SA-AKI, is now recognized as a crucial factor. During sepsis, inflammatory mediators are released from blood vessels and bind to membrane-bound pattern recognition receptors, such as Toll-like receptors, stimulating a cascade of downstream signals that result in the synthesis and release of proinflammatory molecules (Dellepiane et al., 2016; Fry, 2012; Hotchkiss & Karl, 2003; Kalakeche et al., 2011; Peerapornratana et al., 2019). Another critical component for organ function is adequate tissue perfusion. In SA-AKI, there is a notable reduction in capillary density, marked by a decrease in capillaries with continuous flow and an increase in those with intermittent and halted flow (Peerapornratana et al., 2019). The microcirculatory dysfunction can result from multiple factors, including endothelial injury and autonomic nervous system dysregulation. In addition, SA-AKI is implicated in metabolic reprogramming of renal tubular epithelial cells. Prevailing theories suggest that this reprogramming is largely driven by mitochondrial processes, characterized by optimization of energy expenditure, reprogramming of substrate utilization, and mitigation of pro-apoptotic triggers (Peerapornratana et al., 2019).

Cardiorenal syndrome type 1 (CRS-1)-induced kidney injury models

CRS-1 is a multifactorial syndrome characterized by acute renal insufficiency resulting from acute heart failure, often accompanied by myocardial and/or renal hemodynamic changes. The pathophysiological mechanisms of acute heart failure or acutely decompensated chronic heart failure leading to AKI are diverse and complex. Several experimental models of CRS-1 have been developed, including the acute myocardial infarction, cardiac arrest, and cardiopulmonary bypass models, to study the complex mechanisms underlying CRS-1 and provide insights into the hemodynamic changes that contribute to AKI in the context of acute heart failure. The selection of a specific model depends on the particular aspects of CRS-1 that researchers aim to explore.

Acute myocardial infarction (AMI) model: To establish the AMI model, animals are first anesthetized, and an incision is made along the 3rd to 4th intercostal level on the left side of the chest. Subcutaneous tissues and muscles are carefully separated to expose the heart. The left anterior descending coronary artery is then ligated approximately 2 mm below the lower margin of the left auricle using a 7-0 silk suture. Successful establishment of AMI is confirmed by decreased myocardial motion, myocardial pallor, and a 0.2 mV elevation of the ST segment on an electrocardiogram. Finally, the chest is sutured in layers, and any residual air is expelled from the chest cavity. The sham operation group undergoes the same procedure without the coronary artery ligation (Chang et al., 2018). AMI induction increases SCr and BUN levels, renal hypoxia, and inflammatory responses (Hukriede et al., 2022), with long-term observations showing a decrease in eGFR and an increase in renal fibrosis. However, whether these changes indicate a progression from AKI to CKD remains unknown (Hukriede et al., 2022).

Cardiac arrest model: To establish the cardiac arrest model, animals are first anesthetized and placed in a supine position, before being mechanically ventilated at a rate of 150 beats per minute (bpm), with their heart rate maintained between 400–500 bpm. After the chest hair is removed and the area is sterilized with 75% alcohol, a 30-gauge puncture needle is carefully inserted through the intercostal space into the left ventricle under ultrasound guidance. Cardiac arrest is immediately induced by injecting 40 μL of 0.5 mol/L potassium chloride solution, preheated to 37°C, into the left ventricular cavity. The ventilator is then turned off, and Doppler imaging is used to confirm the absence of blood flow in the aortic outflow tract, verifying cardiac arrest. Subsequently, another 30-gauge needle is inserted into the left ventricle to administer 500 μL of

15 μg/mL saline (37°C) epinephrine over approximately 30 seconds, with the mice remaining in cardiac arrest for approximately 7.5 minutes. At the 8 minute mark, mechanical ventilation is resumed at a rate of 180 bpm, and cardiopulmonary resuscitation (CPR) is initiated. The return of spontaneous circulation (ROSC) is then evaluated. If sinus rhythm is detected, Doppler imaging is conducted to confirm aortic flow. If ROSC is not achieved, one or two additional 1-minute cycles of CPR are carried out. Animals that fail to achieve ROSC within 3 minutes are euthanized (Rutledge et al., 2020).

This model presents significant surgical challenges but is capable of inducing severe AKI, characterized by near-zero GFR at 24 hours (Lan et al., 2012), elevated urinary NGAL and renal KIM-1 levels, PTEC injury, and inflammatory infiltrates (Hukriede et al., 2022).

Cardiopulmonary bypass (CBP) model: Following anesthesia and intubation, a midline neck incision is made to expose and cannulate the right jugular vein and left carotid artery. After ensuring the correct placement of the cannulae, systemic heparinization is achieved by injecting heparin at a dose of 2.5 IU/g of animal body-weight through the jugular vein. To facilitate real-time invasive pressure monitoring, an additional cannula is inserted into the left femoral artery. Following the successful placement of both arterial and venous cannulae, cardiopulmonary bypass is initiated by starting the pump at a flow rate of 0.5 mL/min, gradually increasing to 4–6 mL/min over a span of 2 minutes to establish stable flow. Under constant supervision, an upper sternotomy is performed and a cross-clamp is applied to induce cardiac arrest (Madrahimov et al., 2017). The model effectively replicates clinical features of AKI, including moderate increases in BUN and SCr, which are attributed to reduced renal perfusion, immune activation, intravascular hemolysis, and dilutional anemia (Sieben & Harris, 2023). However, the long-term outcomes of AKI induced by this model remain unexplored (Hukriede et al., 2022).

Photothrombosis-induced kidney ischemia model

A novel AKI model was recently established using photothrombosis to induce kidney ischemia (Brezgunova et al., 2023). In this model, a Rose Bengal solution (40 mg/kg) is injected into the jugular vein of rats following anesthesia. After the abdomen is exposed and shaved, a vertical incision is made to expose the left kidney. Five minutes after the Rose Bengal injection, a 520 nm laser, precisely positioned 2 mm above the inferior pole of the kidney using a stereotaxic device, is activated for 10 minutes to induce localized ischemic damage. The contralateral kidney remains unaffected (Brezgunova et al., 2023).

In this model, the area of induced kidney injury, as revealed by triphenyltetrazolium chloride (TTC) staining, appears distinctly pale compared to the surrounding tissue. Various staining techniques have confirmed significant renal damage, with elevated levels of injury and proliferation markers such as KIM-1 and proliferating cell nuclear antigen in the damaged region compared to normal tissue. Although this model does not produce a significant rise in BUN and SCr levels, a marked increase in urinary NGAL levels is observed 6 hours post-photothrombosis. In a modified version of the model involving contralateral nephrectomy, significant elevations in BUN and SCr concentrations are detected.

This photothrombosis-based approach offers a reproducible method for creating ischemic lesions, especially in the renal cortex. This technique is straightforward, allows precise localization of the injury, and is minimally invasive, although it does carry a risk of collateral damage. This model also has some limitations, such as restricted infarct size due to limited light penetration and the potential for photothrombotic injury to affect the vessel wall, leading to vasogenic edema. Despite these challenges, the model provides a valuable new tool for studying the pathological processes of AKI.

Kidney organoids

Kidney organoids are sophisticated, autonomous 3D cell aggregations that closely mimic the architecture and function of human kidneys (Nishinakamura, 2019). These organoids represent a significant advancement in nephrology, providing a powerful platform for studying human kidney development and disease, enabling drug screening *in vitro* and the exploration of regenerative therapies (Nishinakamura, 2019).

Since the first successful generation of kidney organoids, many protocols have been developed to induce their formation from human pluripotent stem cells (hPSCs). These protocols rely on the process of “directed differentiation”, where specific growth factors and intermediate agents guide stem cells into forming complex kidney-like structures. Kidney organoids are capable of expressing markers from various nephron segments, including distal tubules, proximal tubules, glomeruli, and podocytes (Bejoy et al., 2022), reflecting their diverse cellular composition. However, these organoids are not without limitations. Their production is expensive, technically challenging, and requires significant expertise. Additionally, there are challenges in scaling up their cultivation for broader applications, and they lack tissue-resident immune cells, which are crucial for fully modeling kidney function and disease response (Bejoy et al., 2022).

Morizane et al. (2015) proposed a superior protocol for cultivating kidney organoids, marking a significant advancement in the field. The protocol begins with the use of the glycogen synthase kinase-3β (GSK-3β) inhibitor CHIR99021 (CHIR) (10 μmol/L) in combination with Noggin (5 ng/mL) for 4 days, followed by the application of activin (10 ng/mL) over 3 days and fibroblast growth factor 9 (FGF9) (10 ng/mL) over 7 days. Subsequently, the cells are transferred to low-attachment plates, where they undergo further culture with a reduced concentration of CHIR (3 μmol/L) for 2 days from day 9, with FGF9 discontinued from day 14. Through this carefully orchestrated differentiation process, nephron progenitor cells (NPCs) in suspension culture develop into 3D kidney organoids, forming organized, multi-component nephron-like structures that closely resemble the nephron (Figure 2). In addition, Nishinakamura (2019) established the “Taguchi protocol”, which first requires extended exposure to a high concentration of CHIR to drive the progression of the posterior nascent mesoderm. Subsequently, a mixture of retinoic acid, activin, bone morphogenetic protein 4, and an intermediate concentration of CHIR is administered to facilitate the transformation of the posterior nascent mesoderm into the posterior intermediate mesoderm. Finally, treatment with FGF9 and a low concentration of CHIR is carried out, leading to the generation of NPCs capable of differentiating into podocytes, cells of the Bowman’s capsule, and tubule epithelial cells. Kroll et al. (2023) also established the immune-infiltrated kidney organoid-on-chip model by differentiating hPSCs into organoids, transplanting them onto adherent

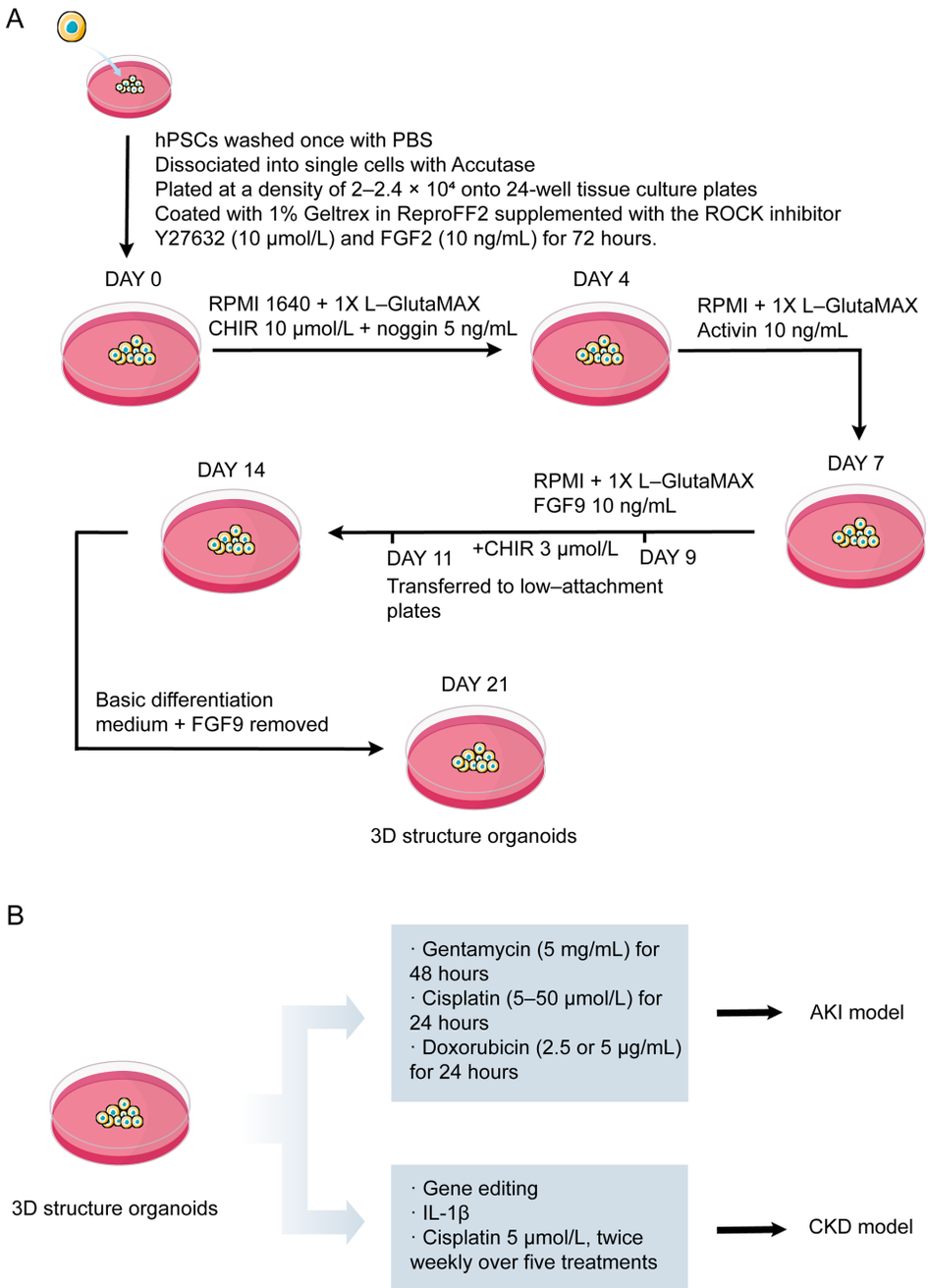

Figure 2 Kidney organoids

A: Protocol for induction of kidney organoids by Morizane et al. (2015). B: Kidney organoid models used to study AKI and CKD via the addition of different reagents or gene editing.

extracellular matrix (ECM), and then introducing circulating peripheral blood mononuclear cells (PBMCs) and T cell bispecific antibodies (TCBs).

Kidney organoids have emerged as important tools for studying the development and pathology of human kidneys, offering a distinct advantage over traditional animal models, which often fail to fully replicate the complexity of human renal diseases. In contrast, kidney organoids derived from hPSCs can be tailored to reflect patient-specific profiles, making them highly valuable for personalized medicine. Their small size and genetic plasticity also make them an ideal platform for the development of high-throughput therapeutic screening (Hukriede et al., 2022).

Kidney organoids have proven successful in modeling AKI induced by various nephrotoxic drugs that exert renal cell-specific effects. For instance, after 21 days of differentiation, kidney organoids treated with gentamycin (5 mg/mL) for 48 hours show a dose-dependent up-regulation of KIM-1 in the tubules, indicating damage to proximal tubular cells (Morizane et al., 2015). Similarly, when exposed to cisplatin (5–50 μmol/L) for 24 hours, 3D Transwell or suspension kidney organoids exhibit significant KIM-1 up-regulation and E-cadherin down-regulation in tubules (Freedman et al., 2015; Morizane et al., 2015; Soo et al., 2018; Takasato et al., 2015). Furthermore, doxorubicin, which is known to damage podocytes and tubular epithelial cells in glomeruli (Bejoy et al., 2022), has been used to induce AKI in kidney organoids following exposure to concentrations of 2.5 or 5 μg/mL for 24 hours (Kumar et al., 2019). These findings underscore the effectiveness of kidney organoids as a robust, patient-specific

platform for evaluating the nephrotoxicity of drugs and other chemical substances, providing critical insights into renal pathology and potential therapeutic interventions.

CHRONIC KIDNEY DISEASE

CKD models can be categorized based on the underlying etiology of the disease, including 5/6 nephrectomy, unilateral ureteral obstruction (UUO), post-AKI, primary kidney disease, secondary disease, and hereditary kidney disease models (Figure 3). While rodent models remain the most frequently utilized, there is growing interest in the use of renal organoids for simulating CKD.

5/6 nephrectomy model

The standard 5/6 nephrectomy model is established with an initial flank incision to expose the right kidney. One week later, another flank incision is made to surgically excise the upper and lower poles of the left kidney. By postoperative week 4, mice subjected to 5/6 nephrectomy exhibit significantly elevated SCr, BUN, and proteinuria levels compared to sham-operated controls (Tan et al., 2019). This model mimics the glomerular structural changes observed in CKD, with severe reductions in kidney mass by week 2, and focal segmental glomerulosclerosis lesions appearing in over 50% of glomeruli by week 7 (Yang et al., 2018). However, this model carries the risk of complications such as massive renal hemorrhage and infection, which can increase postoperative mortality (Tan et al., 2019).

UUO model

The UUO model serves as a classic model for studying obstructive nephropathy. It involves anesthetizing the animal and making a vertical incision approximately 1 cm in length along the abdomen or flank. The ureter is then carefully isolated, bluntly separated, and ligated with a silk suture. Male rats are generally preferred for this model due to the potential complications posed by the more complex reproductive anatomy of female rats. In the UUO model, a decrease in GFR is detectable within 24 hours, followed by tubular dilatation, interstitial inflammatory cell infiltration, and tubular cell death via apoptosis and necrosis over the subsequent days. This progression leads to severe hydronephrosis and significant renal parenchymal loss within 1–2 weeks, ultimately resulting in renal fibrosis (Chevalier et al., 2009). The key mechanisms driving this process involve the nuclear factor kappa B (NF-κB) and mitogen-activated protein kinase (MAPK) pathways, with ongoing research focused on the development of targeted therapies (Martínez-Klimova et al., 2019).

Post-AKI models

AKI plays an important role in the onset and advancement of CKD. The severity and frequency of AKI significantly influence the likelihood of transitioning to CKD. In AKI pathology, the surviving renal tubular epithelial cells typically proliferate and initiate renal repair. Ideally, this repair process restores tubular epithelial integrity and function; however, incomplete or maladaptive repair can lead to the development of CKD (Fu et al., 2018). Despite rapid advancements, the precise mechanisms driving AKI-CKD transition remain unclear.

IR-induced model: Multiple IR models have been employed to investigate the mechanisms underlying CKD, including bilateral IR, unilateral IR, and repeated IR models. For example, Yang et al. (2010) conducted experiments on BALB/c mice, subjecting them to either moderate IR injury with

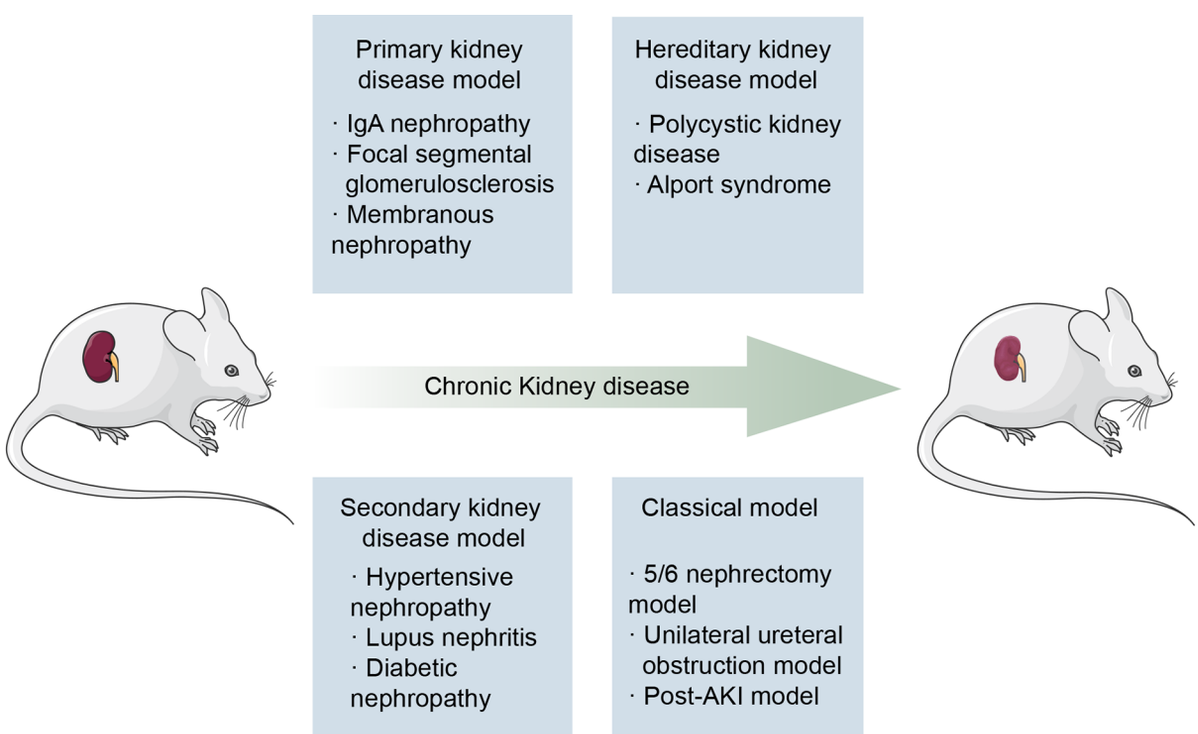

Figure 3 Common causes of chronic kidney disease (CKD)

Common causes of CKD include primary kidney diseases such as IgA nephropathy, FSGS, and membranous nephropathy. Secondary kidney diseases that often lead to CKD include hypertensive nephropathy, lupus nephritis, and diabetic nephropathy. Hereditary kidney disease models frequently used in CKD research include polycystic kidney disease and Alport syndrome models. Traditional animal modeling approaches for CKD include 5/6 nephrectomy, UUO, and post-AKI models.

bilateral renal artery clamping for 30 minutes at 37°C or severe IR injury with bilateral renal artery clamping for 32 minutes at 37.5°C. In the severe IR group, SCr levels remained elevated 42 days post-injury, with the kidneys developing chronic changes characterized by tubulointerstitial fibrosis, indicative of AKI-CKD transition. Zhang et al. (2020) advanced a novel CKD model using a bilateral IR approach, performing a two-stage IR surgery where the renal artery of the left kidney was first clamped, followed by the same procedure on the right kidney 14 days later. This sequential severe IR injury often leads to insufficient recovery from ischemic AKI, progressing to CKD (Zhang et al., 2020). In addition, unilateral IR models are also commonly used in post-AKI research (Lech et al., 2014; Lech et al., 2013; Zager et al., 2011). In these models, the contralateral kidney remains intact and functional, enabling long-term survival of the animals while modeling CKD.

Drug and toxin-induced model: Various studies have administered repeated low doses of nephrotoxic drugs, such as cisplatin, aristolochic acid (AA), and diphtheria toxin (DT), to establish CKD models. Cisplatin is typically given at doses of 10 mg/kg or less, administered weekly or biweekly over a period of 3–4 weeks, and has been shown to result in the development of tubulointerstitial fibrosis and elevated fibrotic markers (TGF-β, p-SMAD3, and fibronectin) (Fu et al., 2018; Katagiri et al., 2016; Pabla et al., 2011; Sharp et al., 2016). In a different approach, Grgic et al. (2012) used genetically modified bigenic *Six2-GFP*$^{Cre+}$*-iDTR*$^{+}$ mice to specifically target renal epithelial cells for diphtheria toxin-induced injury. By administering sublethal doses of DT (0.15 μg/kg) three times over one-week, they induced injury to the S1 and S2 segments of the proximal tubular epithelial cells, resulting in maladaptive repair, characterized by interstitial fibrosis and capillary loss. The proximal tubular damage in the renal cortex resulted in chronic tubulointerstitial damage with varying degrees of renal tubular atrophy and interstitial fibrosis. Animals with advanced tubulointerstitial injury exhibited elevated SCr levels, indicating significant renal dysfunction (Grgic et al., 2012). Further reinforcing the utility of DT in CKD modeling, Takaori et al. (2016) established a similar DT-induced CKD model using doses of 0.25 ng/g, resulting in characteristic features of CKD, including tubular glomeruli, fibrosis, and glomerulosclerosis. CKD mouse models have also been developed via intraperitoneal administration of AA (3.5 mg/kg) over 4 consecutive days, resulting in significant renal damage and histopathological features at 5, 10, and 25 days post-administration, including interstitial cell infiltration and tubulointerstitial fibrosis (Jadot et al., 2017).

Primary kidney disease models

Primary kidney diseases encompass a group of distinct conditions originating within the kidneys, often with unclear etiologies, although they are frequently associated with autoimmune dysfunction. These diseases display notable ethnic variations and genetic predispositions and are a major contributor to CKD. CKD is diagnosed when primary kidney disease persists for more than 3 months, leading to progressive or irreversible deterioration of renal structure and function.

IgA nephropathy (IgAN): IgAN is the most prevalent form of primary glomerulonephritis worldwide. The prognosis for this disease is generally poor, and no definitive treatment has been established, primarily due to the complex and poorly understood pathogenesis of the disease. Research models for IgAN are categorized into non-genetic models, spontaneous IgAN models, and transgenic and humanized mouse models.

The first IgAN model, developed by Rifai et al. (1979), involved injecting murine anti-dinitrophenol (DNP) and DNP-conjugated bovine serum albumin (DNP-BSA), but it was later found that maintaining persistent mesangial immune complex deposition required repeated administration of these agents or sustained high levels of serum immune complexes (Monteiro & Suzuki, 2021). IgAN models have also been developed via oral immunization with *Haemophilus parainfluenzae* or viral infection with parvo and Sendai viruses. Suzuki et al. (2014) successfully established a 100% onset model of spontaneous IgAN (grouped ddY mice: gddY) by interbreeding early-onset mice, which subsequently developed proteinuria by 8 weeks of age, along with mesangial IgA deposition and glomerular damage. However, due to the substantial structural differences between human and rodent IgA, creating reproducible models has proven challenging (Monteiro & Suzuki, 2021). To address these difficulties, researchers have been working on developing transgenic and humanized mouse models. Notably, Berthelot et al. (2012) established a fully humanized IgAN mouse model by backcrossing human *IgA1* knock-in mice with human *CD89* transgenic mice, resulting in α1KICD89Tg mice. By 12 weeks of age, these mice exhibited significant albuminuria, hematuria, impaired renal function, and serum complexes containing human IgA1 and sCD89.

Focal segmental glomerulosclerosis (FSGS): FSGS is a prevalent primary glomerular disease that affects both children and adults with nephrotic syndrome. It is characterized by segmental glomerular scarring with or without intracapillary foam cell formation and adhesions within the glomerular capillaries.

The 5/6 nephrectomy and podocyte toxin-induced models are major animal models used to study FSGS, although their effectiveness may be influenced by the genetic backgrounds of the mice (Yang et al., 2018). Podocyte toxin-induced models can be created by a single injection of puromycin aminonucleoside (50 mg/kg) or by multiple injections of puromycin aminonucleoside (10 mg/kg for first dose, followed by 40 mg/kg every 4 weeks) in conjunction with unilateral nephrectomy, leading to observable glomerulosclerosis by week 8 (Yang et al., 2018). Adriamycin (ADR)-induced nephropathy is also a key model for studying human primary FSGS, as it replicates the common pathways of podocyte injury and glomerular dysfunction that lead to CKD. The model is usually established through a single injection of ADR, with the dosage being highly dependent on the experimental species (Yang et al., 2018). For instance, administering 10 mg/kg ADR to C57BL/6 mice is sufficient to induce FSGS (Dan Hu et al., 2023). Spontaneous FSGS models have been established in Buffalo/Mna rats and Munich-Wistar-Fromter rats, while genetically engineered FSGS models have also been developed, including those targeting podocyte expression molecules, such as α-Actinin 4 knockout (Kos et al., 2003; Michaud et al., 2003; Yao et al., 2004), laminin beta2 knockout (Suh et al., 2011), and transient receptor potential channel 6 transgenic models (Krall et al., 2010).

Membranous nephropathy (MN): Membranous nephropathy is the leading cause of nephrotic syndrome in adults, characterized by the deposition of immune complexes on the epithelial side of the glomerulus (Wang et al., 2024). This

condition ultimately leads to a variety of clinical manifestations, such as proteinuria, hematuria, edema, and hypertension (Kodner, 2009; Politano et al., 2020). Passive Heymann nephritis models, frequently employed to study MN (Bao et al., 2018), have been induced in male rats via intraperitoneal injection of anti-Fx1A serum at a dose of 5 to 6 mL/kg (Di Tu et al., 2020; Schubart et al., 2019). More recently, Meyer-Schwesinger et al. (2020) introduced an *mPLA2R1* knock-in mouse model, which develops MN-like features, including the formation of subepithelial immune complexes, complement activation, and subsequent proteinuria.

Secondary kidney disease models

Secondary kidney disease is a significant and growing contributor to CKD, with its incidence increasing each year. This condition arises when kidney damage is caused by diseases affecting other systems, often presenting with features specific to the primary underlying disease.

Hypertensive nephropathy: Hypertension is a prevalent risk factor for the onset of chronic cardiovascular diseases, such as hypertensive nephropathy. Within the glomerulus, hypertension leads to the damage and activation of mesangial cells, resulting in the secretion of substantial quantities of vasoactive and proinflammatory factors (Lucero et al., 2022). Research on hypertensive nephropathy has made significant strides in recent years. For instance, (Gelosa et al., 2013) established a hypertensive nephropathy model in rats be providing a permissive diet supplemented with 1% NaCl in drinking water, with subsequent analysis showing a progressive increase in 24-hour proteinuria after 4 weeks and significantly higher SCr levels after 5 weeks. Hypertensive nephropathy has also been modeled using continuous angiotensin II (AngⅡ) infusion (1.46 mg/kg) via an osmotic minipump over 28 days (Ding et al., 2019; Liu et al., 2014), resulting in marked increases in SCr and BUN levels as well as biomarkers of renal fibrosis and proinflammatory cytokines (Ding et al., 2019). However, a recent study indicated that the histopathological changes observed in AngⅡ-infused mice resemble mesangioproliferative glomerulonephritis rather than typical hypertensive nephropathy (Gutsol et al., 2022), suggesting that more accurate models are needed to better characterize this disease.

Lupus nephritis (LN): LN is a common and serious complication of systemic lupus erythematosus (SLE), significantly contributing to the overall morbidity and mortality associated with the disease (Almaani et al., 2017). Among the various models used to study LN, spontaneous models are the most prevalent, including F1 hybrids (NZB/WF1) derived from New Zealand Black (NZB) and New Zealand White (NZW) mice, Murphy Roths Large/lymphoproliferative (MRL/lpr) mice, BXSB mice, and their progeny (Xin et al., 2022). In NZB/WF1 mice, antibodies against dsDNA, histone H1, histone H2A, chromatin, and ribonucleoproteins begin to appear at 2–4 months of age and persist for long periods, consistent with the chronic nature of the disease in humans (Drake et al., 1995). Immune complex deposition-mediated glomerulonephritis develops by 4–6 months, followed by severe proteinuria at 8–10 months. The mice typically have a lifespan of approximately 10 months, ultimately succumbing to renal failure (Bagavant et al., 2020). In contrast, MRL/lpr mice develop a more rapidly progressing lupus-like disease, with disease onset occurring around 8 weeks of age (Xin et al., 2022), with proliferative glomerulonephritis characterized by endothelial and mesangial cell proliferation and crescent formation (Cohen & Eisenberg, 1991). BXSB mice, particularly males, present with elevated antinuclear antibody (ANA) levels by 2–3 months (Xin et al., 2022) and develop acute to subacute, proliferative, and exudative glomerulonephritis (Andrews et al., 1978). In addition to spontaneous models, genetically engineered models have been developed by altering specific genes in wild-type mice, including *B6.Tlr7.Tg* and *B6.Fcgr2b*$^{-/-}$ mice (Bolland & Ravetch, 2000; Cheung et al., 2009; Deane et al., 2007). Immune tolerance is disrupted in knockout and transgenic models via modification of key immunological processes (Xin et al., 2022). Drug-induced models, especially pristane-induced models, have also been used in research (Chen et al., 2020).

Diabetic nephropathy (DN): Although DN is a significant contributor to end-stage renal disease, the development of effective therapies is hindered by the lack of rodent models that fully replicate the human condition. The Animal Models of Diabetic Complications Consortium has established key criteria for optimal rodent models of DN, including evident albuminuria, histopathological indications of glomerulosclerosis, and a gradual decline in kidney function (Azushima et al., 2018).

One widely used model for studying type 1 diabetes mellitus (T1DM) is induced by streptozotocin (STZ), a chemical toxin that selectively targets pancreatic β-cells. Diabetes can be induced in mice by administering multiple low doses of STZ (40 mg/kg, intraperitoneally) over 5 consecutive days or by a single high dose of STZ (200 mg/kg), which is directly toxic to pancreatic β-cells, causing rapid-onset diabetes, with blood glucose concentrations exceeding 500 mg/dL within 48 hours. The use of multiple low doses of STZ is preferred because it mimics the chronic pancreatic islet inflammation, insulitis, and insulin deficiency observed in human T1DM (Azushima et al., 2018). For modeling type 2 diabetes mellitus (T2DM), researchers often use a combination of high-fat diet (HFD) feeding and STZ injections. In this model, mice are fed either an HFD (60% of calories from fat) or a standard chow diet (10% of calories from fat) for 24 weeks. At week 23, mice are injected with 40 mg/kg STZ daily for 3 consecutive days to induce T2DM. However, some studies have found that diabetes induced by low-dose STZ administration can result in only mild kidney injury, even in permissive strains, with evidence suggesting that renal lesions may be due to the direct nephrotoxic effects of STZ itself (Gurley et al., 2006; Qi et al., 2005). Genetic models of T1DM, such as Akita and OVE26 mice, have also been utilized in DN research. Akita^{Ins2+} mice carry a spontaneous point mutation in the preproinsulin gene, leading to β-cell dysfunction and death (Giralt-Lopez et al., 2020). These mice develop renal impairment and elevated serum IgA, although the effects are more pronounced in male mice than in female mice (Kitada et al., 2016). OVE26 mice, which overexpress calmodulin in pancreatic β-cells, can develop severe diabetes within the first week of life (Azushima et al., 2018).

Classical models of T2DM include diet-induced models, as well as genetically modified mice, such as leptin receptor-deficient (*db/db*) or leptin-deficient (*ob/ob*) strains, and the New Zealand Obese (NZO/H1Lt) model. While genetically manipulated models improve model quality, dietary models that incorporate high-fat and/or high-sugar diets better mimic human T2DM characteristics, often combined with disease-

promoting factors such as STZ injection (Preguiça et al., 2020). However, these methods often fail to produce substantial renal injury in certain rodent strains, with the extent of renal involvement typically limited to mild albuminuria and minimal glomerulosclerosis, falling short of fully replicating all the features of DN (Giralt-López et al., 2020). To address these limitations, researchers have sought to improve traditional models by backcrossing to diabetic-susceptible backgrounds and employing genetic modifications, including knockout and transgenic techniques. Notable examples include *ob/ob* (leptin-deficient) mice (Clee et al., 2005), endothelial nitric oxide synthase (*eNOS*)$^{-/-}$ models (Mohan et al., 2008; Zhao et al., 2006), models combining STZ or OVE26 transgene with TTRhRen mice (Thibodeau et al., 2014), and hyperreninemic rat models such as CYP1a1mRen2 (Conway et al., 2014). In contrast to C57BL/6 mice, BTBR *ob/ob* mice develop fasting hyperinsulinemia even on a standard mouse chow. Diabetes onset is progressive, with most female BTBR *ob/ob* mice developing insulin resistance by 6 weeks of age, and being decompensated at 14 weeks of age —a process that is accelerated in males (Clee et al., 2005). These mice exhibit significant albuminuria and severe DN pathology, such as extensive mesangial matrix expansion, focal nodular glomerulosclerosis, mild glomerular basement membrane (GBM) thickening, and arteriolar hyalinosis (Azushima et al., 2018). Similarly, *eNO*$^{-/-}$ mice display pronounced albumin excretion, along with extensive mesangial matrix expansion, nodule lesions, increased GBM thickness, arteriolar hyalinosis, and tubulointerstitial fibrosis (Azushima et al., 2018). However, these mice also form atubular nephrons with a marked developmental kidney phenotype, raising questions about whether this model accurately mimics human diabetes (Alpers & Hudkins, 2011). In other models, administering low-dose STZ to TTRhRen mice (HD-STZ mice) or crossbreeding with OVE26 diabetic mice (HD-OVE mice) results in extensive mesangial matrix expansion, tubulointerstitial fibrosis, and other features of advanced DN (Thibodeau et al., 2014).

Hereditary kidney disease models

Hereditary kidney diseases encompass a broad range of genetically linked disorders with diverse etiologies, which potentially affect not only the kidneys but other organs such as the eyes, ears, and bones. Approximately 10% of patients requiring renal replacement therapy are affected by hereditary kidney diseases (Mehta & Jim, 2017). These diseases often progress gradually, with many cases eventually evolving into CKD or advancing to end-stage renal disease. Early genetic diagnosis and targeted treatment are crucial for preventing the progression to CKD.

Polycystic kidney disease (PKD): PKD is an inherited disorder characterized by the formation and enlargement of numerous fluid-filled cysts in the kidneys, which can lead to kidney failure. Despite ongoing research on the pathogenesis and treatment of PKD, there is still a lack of rodent models that can fully simulate human PKD. Pure heterozygotes, such as *PKD1*$^{-/-}$ and *PKD2*$^{-/-}$ mice, do not survive, making it challenging to study the disease (Lu et al., 1997; Wu et al., 2000). As a result, research has shifted toward conditional and gene dosage models (Sieben & Harris, 2023). In gene dosage models, biallelic assessment is used to reduce functional protein levels without complete loss (Sieben & Harris, 2023). For example, Arroyo et al. (2021) established and characterized the *PKD1*$^{RC/RC}$ model, where the onset and severity of clinical signs, such as renal cysts, renal fibrosis, and elevated BUN, vary depending on the genetic backgrounds of the mice (Arroyo et al., 2021). Conditional and inducible models have also been developed, such as *PKD1*$^{fl/-}$, *PKD1*$^{fl/fl}$, *Cdh16*^{cre}*/ERT2*, *Mx1*^{cre}, and *Cag*^{cre}*/ER*, where the insertion of targeted sequences is triggered by specific recombinases (Sieben & Harris, 2023).

Alport syndrome (AS): AS is a hereditary glomerular basement membrane disorder, characterized by hematuria, progressive sensorineural deafness, and ocular abnormalities. The disease arises from mutations in the genes encoding IV collagen, the major collagen component of the glomerular basement membrane. Mutations in the *COL4A3*, *COL4A4*, or *COL4A5* genes lead to the development of AS lesions, and animal models have increasingly focused on alterations in these genes. To date, approximately 15 mouse models have been generated using six different genetic modification techniques, including gene knockout, domain substitutions, nonsense mutations, mutations affecting splice donor sites, missense mutations, and replacement of amino acids with small peptides (Nikolaou & Deltas, 2022). Among these, the *Col4a3* knockout models are the most widely used. Recently, Namba et al. (2021) established a novel AS rat model based on deletion of the *Col4α5* gene by genome editing via oviductal nucleic acid delivery (rGONAD) technology.

Kidney organoids

Kidney organoid models have become a valuable tool in studying CKD, particularly in investigating the mechanisms underlying renal fibrosis, a slowly progressive condition often seen in kidney disease. Researchers are actively working to replicate this process in kidney organoids, as they provide a well-controlled *in vitro* environment that allows for the detailed study of tissue-specific cell signaling and intercellular crosstalk, free from the systemic signals and immune cells present *in vivo* (Moran-Horowich & Lemos, 2021). For example, Lemos et al. (2018) demonstrated that stimulating human kidney organoids with interleukin 1β (IL-1β) induced tubulointerstitial fibrosis with αSMA^{+} myofibroblast activation and collagen deposition, highlighting IL-1β as a potential therapeutic target in tubulointerstitial diseases. Additionally, the up-regulation of pivotal biomarkers, such as NGAL, following IL-1β treatment aligns with observations from animal models and human studies (Hoste et al., 2018; Lan et al., 1995). Kidney organoids have also been used to study nephrotoxic drug-induced CKD. For example, Gupta et al. (2022) treated kidney organoids with cisplatin (5 μmol/L) twice weekly for a total of five treatments and identified homology-directed repair as the mechanism underpinning intrinsic tubular repair, even in the absence of potential anti-fibrotic effects in this model.

Kidney organoids have become an essential tool in studying hereditary kidney diseases, particularly PKD. In research focusing on PKD, *PKD1* and *PKD2* are inactivated by gene editing, leading to the formation of cysts that can be observed as early as day 15. The density at which cells are seeded plays a crucial role in cyst formation (Tran et al., 2022). Cyclic AMP (cAMP) signaling has been identified as a significant contributor to PKD, with its elevation being a cellular hallmark of PKD organoids (Low et al., 2019). Cruz et al. (2017) also highlighted the importance of polycystin-1, a regulator of cell adhesion, in maintaining tubular architecture through cellular

interactions, emphasizing its central role in PKD pathology.

Kidney organoids have also been used to study nephronophthisis (NPHP)-related ciliopathy. NPHP is an autosomal recessive cystic kidney disease. By comparing organoids derived from NPHP-predisposed patients with isogenic control organoids generated from genetically corrected induced PSCs (iPSCs), Forbes et al. (2018) demonstrated the underlying pathology of NPHP. Patient-derived organoid tubules exhibit shortened, rod-like primary cilia, a phenotype that can be corrected through genetic modification. Kidney organoids have also been employed in research on other inherited kidney diseases, such as congenital nephrotic syndrome (Hale et al., 2018; Trautmann et al., 2015) and congenital renal malformations linked to paired box 2 gene defects (Kaku et al., 2017).

CONCLUSIONS

Advancement of diagnostic and therapeutic strategies for kidney disease relies heavily on the development and refinement of various disease models. As discussed above, each model possesses unique strengths and limitations. However, many existing models still face significant challenges, including the inability to fully replicate human kidney disease and the difficulty in capturing the complexity of human AKI pathophysiology. As such, there remains a pressing need to develop more stable and reproducible models of AKI, while CKD research requires models that are compatible with complex and specific pathological changes, likely involving the field of genetic modification. Moreover, emerging approaches such as organoids and organ-on-chip systems, which utilize microfluid platforms and *in vitro* cell culture, represent cutting-edge technologies that hold significant potential for continued research and development.

COMPETING INTERESTS

The authors declare that they have no competing interests.

AUTHORS' CONTRIBUTIONS

W.L. and F.H. contributed to the conception and design of the work; J.M. and H.Z. drafted the manuscript; J.W., J.C., F.H., and W.L. substantively revised the manuscript. All authors read and approved the final version of the manuscript.

REFERENCES

Abou Taka M, Dugbartey GJ, Sener A. 2022. The optimization of renal graft preservation temperature to mitigate cold ischemia-reperfusion injury in kidney transplantation. *International Journal of Molecular Sciences*, **24**(1): 567.

Almaani S, Meara A, Rovin BH. 2017. Update on lupus nephritis. *Clinical Journal of the American Society of Nephrology*, **12**(5): 825–835.

Alpers CE, Hudkins KL. 2011. Mouse models of diabetic nephropathy. *Current Opinion in Nephrology and Hypertension*, **20**(3): 278–284.

Andrassy KM. 2013. Comments on 'KDIGO 2012 clinical practice guideline for the evaluation and management of chronic kidney disease'. *Kidney International*, **84**(3): 622–623.

Andrews BS, Eisenberg RA, Theofilopoulos AN, et al. 1978. Spontaneous murine lupus-like syndromes. Clinical and immunopathological manifestations in several strains. *Journal of Experimental Medicine*, **148**(5): 1198–1215.

Aparicio-Trejo OE, Avila-Rojas SH, Tapia E, et al. 2020. Chronic impairment of mitochondrial bioenergetics and β-oxidation promotes experimental AKI-to-CKD transition induced by folic acid. *Free Radical Biology and Medicine*, **154**: 18–32.

Arroyo J, Escobar-Zarate D, Wells HH, et al. 2021. The genetic background significantly impacts the severity of kidney cystic disease in the *Pkd1*$^{RC/RC}$ mouse model of autosomal dominant polycystic kidney disease. *Kidney International*, **99**(6): 1392–1407.

Azushima K, Gurley SB, Coffman TM. 2018. Modelling diabetic nephropathy in mice. *Nature Reviews Nephrology*, **14**(1): 48–56.

Bagavant H, Michrowska A, Deshmukh US. 2020. The NZB/WF1 mouse model for Sjögren's syndrome: A historical perspective and lessons learned. *Autoimmunity Reviews*, **19**(12): 102686.

Baghdadi M, Chiba S, Yamashina T, et al. 2012. MFG-E8 regulates the immunogenic potential of dendritic cells primed with necrotic cell-mediated inflammatory signals. *PLoS One*, **7**(6): e39607.

Bao YW, Yuan Y, Chen JH, et al. 2018. Kidney disease models: tools to identify mechanisms and potential therapeutic targets. *Zoological Research*, **39**(2): 72–86.

Bejoy J, Qian ES, Woodard LE. 2022. Tissue culture models of AKI: From tubule cells to human kidney organoids. *Journal of the American Society of Nephrology*, **33**(3): 487–501.

Berthelot L, Papista C, Maciel TT, et al. 2012. Transglutaminase is essential for IgA nephropathy development acting through IgA receptors. *Journal of Experimental Medicine*, **209**(4): 793–806.

Bolland S, Ravetch JV. 2000. Spontaneous autoimmune disease in FcγRIIB-deficient mice results from strain-specific epistasis. *Immunity*, **13**(2): 277–285.

Brezgunova AA, Andrianova NV, Popkov VA, et al. 2023. New experimental model of kidney injury: photothrombosis-induced kidney ischemia. *Biochimica et Biophysica Acta* (*BBA*)-*Molecular Basis of Disease*, **1869**(3): 166622.

Chang D, Wang YC, Xu TT, et al. 2018. Noninvasive identification of renal hypoxia in experimental myocardial infarctions of different sizes by using BOLD MR imaging in a mouse model. *Radiology*, **286**(1): 129–139.

Chen WW, Li WC, Zhang ZY, et al. 2020. Lipocalin-2 exacerbates lupus nephritis by promoting Th1 cell differentiation. *Journal of the American Society of Nephrology*, **31**(10): 2263–2277.

Cheng YT, Tu YC, Chou YH, et al. 2022. Protocol for renal ischemia-reperfusion injury by flank incisions in mice. *STAR Protocols*, **3**(4): 101678.

Cheung YH, Loh C, Pau E, et al. 2009. Insights into the genetic basis and immunopathogenesis of systemic lupus erythematosus from the study of mouse models. *Seminars in Immunology*, **21**(6): 372–382.

Chevalier RL, Forbes MS, Thornhill BA. 2009. Ureteral obstruction as a model of renal interstitial fibrosis and obstructive nephropathy. *Kidney International*, **75**(11): 1145–1152.

Chu C, Delić D, Alber J, et al. 2022. Head-to-head comparison of two SGLT-2 inhibitors on AKI outcomes in a rat ischemia-reperfusion model. *Biomedicine & Pharmacotherapy*, **153**: 113357.

Clee SM, Nadler ST, Attie AD. 2005. Genetic and genomic studies of the BTBR ob/ob mouse model of type 2 diabetes. *American Journal of Therapeutics*, **12**(6): 491–498.

Cohen PL, Eisenberg RA. 1991. *Lpr* and *gld*: single gene models of systemic autoimmunity and lymphoproliferative disease. *Annual Review of Immunology*, **9**: 243–269.

Conway BR, Betz B, Sheldrake TA, et al. 2014. Tight blood glycaemic and blood pressure control in experimental diabetic nephropathy reduces extracellular matrix production without regression of fibrosis. *Nephrology*, **19**(12): 802–813.

Cruz NM, Song XW, Czerniecki SM, et al. 2017. Organoid cystogenesis reveals a critical role of microenvironment in human polycystic kidney disease. *Nature Materials*, **16**(11): 1112–1119.

Deane JA, Pisitkun P, Barrett RS, et al. 2007. Control of toll-like receptor 7 expression is essential to restrict autoimmunity and dendritic cell

proliferation. *Immunity*, **27**(5): 801–810.
Dellepiane S, Marengo M, Cantaluppi V. 2016. Detrimental cross-talk between sepsis and acute kidney injury: new pathogenic mechanisms, early biomarkers and targeted therapies. *Critical Care*, **20**(1): 61.
Di Tu Q, Jin J, Hu X, et al. 2020. Curcumin improves the renal autophagy in rat experimental membranous nephropathy via regulating the PI3K/AKT/mTOR and Nrf2/HO-1 signaling pathways. *Biomed Research International*, **2020**(1): 7069052.
Ding H, Zhou Y, Huang HH. 2019. MiR-101a ameliorates AngII-mediated hypertensive nephropathy by blockade of TGFβ/Smad3 and NF-κB signalling in a mouse model of hypertension. *Clinical and Experimental Pharmacology and Physiology*, **46**(3): 246–254.
Drake CG, Rozzo SJ, Vyse TJ, et al. 1995. Genetic contributions to lupus-like disease in (NZB×NZW)F_1 mice. *Immunological Reviews*, **144**(1): 51–74.
Forbes TA, Howden SE, Lawlor K, et al. 2018. Patient-iPSC-Derived Kidney Organoids Show Functional Validation of a Ciliopathic Renal Phenotype and Reveal Underlying Pathogenetic Mechanisms. Am J Hum Genet, 102(5): 816-831.
Freedman BS, Brooks CR, Lam AQ, et al. 2015. Modelling kidney disease with CRISPR-mutant kidney organoids derived from human pluripotent epiblast spheroids. *Nature Communications*, **6**: 8715.
Fry DE. 2012. Sepsis, systemic inflammatory response, and multiple organ dysfunction: the mystery continues. *American Surgeon*, **78**(1): 1–8.
Fu Y, Tang CY, Cai J, et al. 2018. Rodent models of AKI-CKD transition. *American Journal Of Physiology-renal Physiology*, **315**(4): F1098–F1106.
Gelosa P, Pignieri A, Gianazza E, et al. 2013. Altered iron homeostasis in an animal model of hypertensive nephropathy: stroke-prone rats. *Journal of Hypertension*, **31**(11): 2259–2269.
Giralt-López A, Molina-Van Den Bosch M, Vergara A, et al. 2020. Revisiting experimental models of diabetic nephropathy. *International Journal of Molecular Sciences*, **21**(10): 3587.
Grgic I, Campanholle G, Bijol V, et al. 2012. Targeted proximal tubule injury triggers interstitial fibrosis and glomerulosclerosis. *Kidney International*, **82**(2): 172–183.
Gupta N, Matsumoto T, Hiratsuka K, et al. 2022. Modeling injury and repair in kidney organoids reveals that homologous recombination governs tubular intrinsic repair. *Science Translational Medicine*, **14**(634): eabj4772.
Gurley SB, Clare SE, Snow KP, et al. 2006. Impact of genetic background on nephropathy in diabetic mice. *American Journal of Physiology: Renal Physiology*, **290**(1): F214–F222.
Gutsol AA, Blanco P, Hale TM, et al. 2022. Comparative analysis of hypertensive nephrosclerosis in animal models of hypertension and its relevance to human pathology. Glomerulopathy. *PLoS One*, **17**(2): e0264136.
Hale LJ, Howden SE, Phipson B, et al. 2018. 3D organoid-derived human glomeruli for personalised podocyte disease modelling and drug screening. *Nature Communications*, **9**(1): 5167.
Holditch SJ, Brown CN, Lombardi AM, et al. 2019. Recent advances in models, mechanisms, biomarkers, and interventions in cisplatin-induced acute kidney injury. *International Journal of Molecular Sciences*, **20**(12): 3011.
Hosohata K, Jin DN, Takai S. 2021. In vivo and in vitro evaluation of urinary biomarkers in ischemia/reperfusion-induced kidney injury. *International Journal of Molecular Sciences*, **22**(21): 11448.
Hoste EaJ, Kellum JA, Selby NM, et al. 2018. Global epidemiology and outcomes of acute kidney injury. *Nature Reviews Nephrology*, **14**(10): 607–625.
Hotchkiss RS, Karl IE. 2003. The pathophysiology and treatment of sepsis. *New England Journal of Medicine*, **348**(2): 138–150.
Hu QD, Wang HL, Liu J, et al. 2023. Btg2 promotes focal segmental glomerulosclerosis via smad3-dependent podocyte-mesenchymal transition. *Advanced Science*, **10**(32): 2304360.
Hu ZX, Zhang H, Yi B, et al. 2020. VDR activation attenuate cisplatin induced AKI by inhibiting ferroptosis. *Cell Death & Disease*, **11**(1): 73.
Hukriede NA, Soranno DE, Sander V, et al. 2022. Experimental models of acute kidney injury for translational research. *Nature Reviews Nephrology*, **18**(5): 277–293.
Jadot I, Colombaro V, Martin B, et al. 2017. Restored nitric oxide bioavailability reduces the severity of acute-to-chronic transition in a mouse model of aristolochic acid nephropathy. *PLoS One*, **12**(8): e0183604.
Kaku Y, Taguchi A, Tanigawa S, et al. 2017. *PAX2* is dispensable for *in vitro* nephron formation from human induced pluripotent stem cells. *Scientific Reports*, **7**(1): 4554.
Kalakeche R, Hato T, Rhodes G, et al. 2011. Endotoxin uptake by S1 proximal tubular segment causes oxidative stress in the downstream S2 segment. *Journal of the American Society of Nephrology*, **22**(8): 1505–1516.
Katagiri D, Hamasaki Y, Doi K, et al. 2016. Interstitial renal fibrosis due to multiple cisplatin treatments is ameliorated by semicarbazide-sensitive amine oxidase inhibition. *Kidney International*, **89**(2): 374–385.
Kellum JA, Romagnani P, Ashuntantang G, et al. 2021. Acute kidney injury. *Nature Reviews Disease Primers*, **7**(1): 52.
Kher A, Meldrum KK, Wang MJ, et al. 2005. Cellular and molecular mechanisms of sex differences in renal ischemia-reperfusion injury. *Cardiovascular Research*, **67**(4): 594–603.
Kim DH, Choi HI, Park JS, et al. 2022. Farnesoid X receptor protects against cisplatin-induced acute kidney injury by regulating the transcription of ferroptosis-related genes. *Redox Biology*, **54**: 102382.
Kitada M, Ogura Y, Koya D. 2016. Rodent models of diabetic nephropathy: their utility and limitations. *International Journal of Nephrology and Renovascular Disease*, **9**: 279–290.
Kodner C. 2009. Nephrotic syndrome in adults: diagnosis and management. *American Family Physician*, **80**(10): 1129–1134.
Kos CH, Le TC, Sinha S, et al. 2003. Mice deficient in α-actinin-4 have severe glomerular disease. *Journal of Clinical Investigation*, **111**(11): 1683–1690.
Krall P, Canales CP, Kairath P, et al. 2010. Podocyte-specific overexpression of wild type or mutant trpc6 in mice is sufficient to cause glomerular disease. *PLoS One*, **5**(9): e12859.
Kroll KT, Mata MM, Homan KA, et al. 2023. Immune-infiltrated kidney organoid-on-chip model for assessing T cell bispecific antibodies. *Proceedings of the National Academy of Sciences of the United States of America*, **120**(35): e2305322120.
Kumar G, Solanki MH, Xue XY, et al. 2017. Magnesium improves cisplatin-mediated tumor killing while protecting against cisplatin-induced nephrotoxicity. *American Journal of Physiology: Renal Physiology*, **313**(2): F339–F350.
Kumar SV, Er PX, Lawlor KT, et al. 2019. Kidney micro-organoids in suspension culture as a scalable source of human pluripotent stem cell-derived kidney cells. *Development*, **146**(5): dev172361.
Lan HY, Nikolic-Paterson DJ, Mu W, et al. 1995. Interleukin-1 receptor antagonist halts the progression of established crescentic glomerulonephritis in the rat. *Kidney International*, **47**(5): 1303–1309.
Lan YF, Chen HH, Lai PF, et al. 2012. MicroRNA-494 reduces ATF3 expression and promotes AKI. *Journal of the American Society of Nephrology*, **23**(12): 2012–2023.
Lech M, Avila-Ferrufino A, Allam R, et al. 2009. Resident dendritic cells prevent postischemic acute renal failure by help of single Ig IL-1 receptor-related protein. *The Journal of Immunology*, **183**(6): 4109–4118.
Lech M, Gröbmayr R, Ryu M, et al. 2014. Macrophage phenotype controls long-term AKI outcomes--kidney regeneration versus atrophy. *Journal of the American Society of Nephrology*, **25**(2): 292–304.

Lech M, Römmele C, Gröbmayr R, et al. 2013. Endogenous and exogenous pentraxin-3 limits postischemic acute and chronic kidney injury. *Kidney International*, **83**(4): 647–661.

Lemos DR, Mcmurdo M, Karaca G, et al. 2018. Interleukin-1β activates a MYC-dependent metabolic switch in kidney stromal cells necessary for progressive tubulointerstitial fibrosis. *Journal of the American Society of Nephrology*, **29**(6): 1690–1705.

Li L, Khan MN, Li Q, et al. 2015. G31P, CXCR1/2 inhibitor, with cisplatin inhibits the growth of mice hepatocellular carcinoma and mitigates high-dose cisplatin-induced nephrotoxicity. *Oncology Reports*, **33**(2): 751–757.

Li X, Zou Y, Fu YY, et al. 2021. A-lipoic acid alleviates folic acid-induced renal damage through inhibition of ferroptosis. *Frontiers in Physiology*, **12**: 680544.

Liu GX, Li YQ, Huang XR, et al. 2014. Smad7 inhibits AngII-mediated hypertensive nephropathy in a mouse model of hypertension. *Clinical Science*, **127**(3): 195–208.

Low JH, Li P, Chew EGY, et al. 2019. Generation of human PSC-derived kidney organoids with patterned nephron segments and a *De novo* vascular network. *Cell Stem Cell*, **25**(3): 373–387. e9.

Lu QM, Wang MJ, Gui Y, et al. 2020. Rheb1 protects against cisplatin-induced tubular cell death and acute kidney injury via maintaining mitochondrial homeostasis. *Cell Death & Disease*, **11**(5): 364.

Lu WN, Peissel B, Babakhanlou H, et al. 1997. Perinatal lethality with kidney and pancreas defects in mice with a targetted *Pkd1* mutation. *Nature Genetics*, **17**(2): 179–181.

Lucero CM, Prieto-Villalobos J, Marambio-Ruiz L, et al. 2022. Hypertensive nephropathy: unveiling the possible involvement of hemichannels and pannexons. *International Journal of Molecular Sciences*, **23**(24): 15936.

Madrahimov N, Natanov R, Boyle EC, et al. 2017. Cardiopulmonary bypass in a mouse model: a novel approach. *Journal of Visualized Experiments*, (127): 56017.

Martínez-Klimova E, Aparicio-Trejo OE, Tapia E, et al. 2019. Unilateral ureteral obstruction as a model to investigate fibrosis-attenuating treatments. *Biomolecules*, **9**(4): 141.

Mehta L, Jim B. 2017. Hereditary renal diseases. *Seminars in Nephrology*, **37**(4): 354–361.

Meyer-Schwesinger C, Tomas NM, Dehde S, et al. 2020. A novel mouse model of phospholipase A2 receptor 1-associated membranous nephropathy mimics podocyte injury in patients. *Kidney International*, **97**(5): 913–919.

Michaud JL, Lemieux LI, Dubé M, et al. 2003. Focal and segmental glomerulosclerosis in mice with podocyte-specific expression of mutant α-actinin-4. *Journal of the American Society of Nephrology*, **14**(5): 1200–1211.

Mohan S, Reddick RL, Musi N, et al. 2008. Diabetic eNOS knockout mice develop distinct macro- and microvascular complications. *Laboratory Investigation*, **88**(5): 515–528.

Monteiro RC, Suzuki Y. 2021. Are there animal models of IgA nephropathy?. *Seminars in Immunopathology*, **43**(5): 639–648.

Moran-Horowich A, Lemos DR. 2021. Methods for the study of renal fibrosis in human pluripotent stem cell-derived kidney organoids. *Methods in Molecular Biology*, **2299**: 435–445.

Morizane R, Lam AQ, Freedman BS, et al. 2015. Nephron organoids derived from human pluripotent stem cells model kidney development and injury. *Nature Biotechnology*, **33**(11): 1193–1200.

Namba M, Kobayashi T, Kohno M, et al. 2021. Creation of X-linked Alport syndrome rat model with Col4a5 deficiency. *Scientific Reports*, **11**(1): 20836.

Nikolaou S, Deltas C. 2022. A comparative presentation of mouse models that recapitulate most features of alport syndrome. *Genes*, **13**(10): 1893.

Nishinakamura R. 2019. Human kidney organoids: progress and remaining challenges. *Nature Reviews Nephrology*, **15**(10): 613–624.

Ozkok A, Edelstein CL. 2014. Pathophysiology of cisplatin-induced acute kidney injury. *BioMed Research International*, **2014**: 967826.

Pabla N, Dong GE, Jiang M, et al. 2011. Inhibition of PKCδ reduces cisplatin-induced nephrotoxicity without blocking chemotherapeutic efficacy in mouse models of cancer. *Journal of Clinical Investigation*, **121**(7): 2709–2722.

Peerapornratana S, Manrique-Caballero CL, Gómez H, et al. 2019. Acute kidney injury from sepsis: current concepts, epidemiology, pathophysiology, prevention and treatment. *Kidney International*, **96**(5): 1083–1099.

Politano SA, Colbert GB, Hamiduzzaman N. 2020. Nephrotic syndrome. *Primary Care: Clinics in Office Practice*, **47**(4): 597–613.

Preguiça I, Alves A, Nunes S, et al. 2020. Diet-induced rodent models of diabetic peripheral neuropathy, retinopathy and nephropathy. *Nutrients*, **12**(1): 250.

Qi ZH, Fujita H, Jin JP, et al. 2005. Characterization of susceptibility of inbred mouse strains to diabetic nephropathy. *Diabetes*, **54**(9): 2628–2637.

Ravichandran K, Holditch S, Brown CN, et al. 2018. IL-33 deficiency slows cancer growth but does not protect against cisplatin-induced AKI in mice with cancer. *American Journal of Physiology: Renal Physiology*, **314**(3): F356–F366.

Ravichandran K, Wang Q, Ozkok A, et al. 2016. CD4 T cell knockout does not protect against kidney injury and worsens cancer. *Journal of Molecular Medicine*, **94**(4): 443–455.

Ren Q, Guo F, Tao SB, et al. 2020. Flavonoid fisetin alleviates kidney inflammation and apoptosis via inhibiting Src-mediated NF-κB p65 and MAPK signaling pathways in septic AKI mice. *Biomedicine & Pharmacotherapy*, **122**: 109772.

Rifai A, Jr. Small PA, Teague PO, et al. 1979. Experimental IgA nephropathy. *Journal of Experimental Medicine*, **150**(5): 1161–1173.

Rudman-Melnick V, Adam M, Potter A, et al. 2020. Single-cell profiling of AKI in a murine model reveals novel transcriptional signatures, profibrotic phenotype, and epithelial-to-stromal crosstalk. *Journal of the American Society of Nephrology*, **31**(12): 2793–2814.

Rutledge CA, Chiba T, Redding K, et al. 2020. A novel ultrasound-guided mouse model of sudden cardiac arrest. *PLoS One*, **15**(12): e0237292.

Schubart A, Anderson K, Mainolfi N, et al. 2019. Small-molecule factor B inhibitor for the treatment of complement-mediated diseases. *Proceedings of the National Academy of Sciences of the United States of America*, **116**(16): 7926–7931.

Sharp CN, Doll MA, Dupre TV, et al. 2016. Repeated administration of low-dose cisplatin in mice induces fibrosis. *American Journal of Physiology: Renal Physiology*, **310**(6): F560–F568.

Sharp CN, Doll MA, Megyesi J, et al. 2018. Subclinical kidney injury induced by repeated cisplatin administration results in progressive chronic kidney disease. *American Journal of Physiology: Renal Physiology*, **315**(1): F161–F172.

Shiva N, Sharma N, Kulkarni YA, et al. 2020. Renal ischemia/reperfusion injury: An insight on in vitro and in vivo models. *Life Sciences*, **256**: 117860.

Sieben CJ, Harris PC. 2023. Experimental models of polycystic kidney disease: applications and therapeutic testing. *Kidney360*, **4**(8): 1155–1173.

Singbartl K, Kellum JA. 2012. AKI in the ICU: definition, epidemiology, risk stratification, and outcomes. *Kidney International*, **81**(9): 819–825.

Soo JYC, Jansen J, Masereeuw R, et al. 2018. Advances in predictive in vitro models of drug-induced nephrotoxicity. *Nature Reviews Nephrology*, **14**(6): 378–393.

Street JM, Koritzinsky EH, Bellomo TR, et al. 2018. The role of adenosine 1a receptor signaling on GFR early after the induction of sepsis. *American Journal of Physiology: Renal Physiology*, **314**(5): F788–F797.

Suh JH, Jarad G, VanDeVoorde RG, et al. 2011. Forced expression of laminin β1 in podocytes prevents nephrotic syndrome in mice lacking

laminin β2, a model for Pierson syndrome. *Proceedings of the National Academy of Sciences of the United States of America*, **108**(37): 15348–15353.

Suzuki H, Suzuki Y, Novak J, et al. 2014. Development of animal models of human IgA nephropathy. *Drug Discovery Today: Disease Models*, **11**: 5–11.

Takaori K, Nakamura J, Yamamoto S, et al. 2016. Severity and frequency of proximal tubule injury determines renal prognosis. *Journal of the American Society of Nephrology*, **27**(8): 2393–2406.

Takasato M, Er PX, Chiu HS, et al. 2015. Kidney organoids from human iPS cells contain multiple lineages and model human nephrogenesis. *Nature*, **526**(7574): 564–568.

Tan RZ, Zhong X, Li JC, et al. 2019. An optimized 5/6 nephrectomy mouse model based on unilateral kidney ligation and its application in renal fibrosis research. *Renal Failure*, **41**(1): 555–566.

Thibodeau JF, Holterman CE, Burger D, et al. 2014. A novel mouse model of advanced diabetic kidney disease. *PLoS One*, **9**(12): e113459.

Tran T, Song CJ, Nguyen T, et al. 2022. A scalable organoid model of human autosomal dominant polycystic kidney disease for disease mechanism and drug discovery. *Cell Stem Cell*, **29**(7): 1083–1101. e7.

Trautmann A, Bodria M, Ozaltin F, et al. 2015. Spectrum of steroid-resistant and congenital nephrotic syndrome in children: the PodoNet registry cohort. *Clinical Journal of the American Society of Nephrology*, **10**(4): 592–600.

Wang JN, Nie WY, Xie XS, et al. 2021. MicroRNA-874-3p/ADAM (a disintegrin and metalloprotease) 19 mediates macrophage activation and renal fibrosis after acute kidney injury. *Hypertension*, **77**(5): 1613–1626.

Wang JN, Zhu HH, Miao J, et al. 2024. Bilateral renal ischemia-reperfusion model for acute kidney injury in mice. *Journal of Visualized Experiments*, (204), doi: 10.3791/65838.

Wang MQ, Yang JJ, Fang X, et al. 2024. Membranous nephropathy: pathogenesis and treatments. *MedComm (2020)*. **5**(7): e614.

Wu GQ, Markowitz GS, Li L, et al. 2000. Cardiac defects and renal failure in mice with targeted mutations in Pkd2. *Nature Genetics*, **24**(1): 75–78.

Xin Y, Zhang B, Zhao JP, et al. 2022. Animal models of systemic lupus erythematosus and their applications in drug discovery. *Expert Opinion on Drug Discovery*, **17**(5): 489–500.

Xu ZM, Zhang MJ, Wang WW, et al. 2023. Dihydromyricetin attenuates cisplatin-induced acute kidney injury by reducing oxidative stress, inflammation and ferroptosis. *Toxicology and Applied Pharmacology*, **473**: 116595.

Yan LJ. 2021. Folic acid-induced animal model of kidney disease. *Animal Models and Experimental Medicine*, **4**(4): 329–342.

Yang JW, Dettmar AK, Kronbichler A, et al. 2018. Recent advances of animal model of focal segmental glomerulosclerosis. *Clinical and Experimental Nephrology*, **22**(4): 752–763.

Yang L, Besschetnova TY, Brooks CR, et al. 2010. Epithelial cell cycle arrest in G2/M mediates kidney fibrosis after injury. *Nature Medicine*, **16**(5): 535–543.

Yao JN, Le TC, Kos CH, et al. 2004. α-actinin-4-mediated FSGS: an inherited kidney disease caused by an aggregated and rapidly degraded cytoskeletal protein. *PLoS Biology*, **2**(6): e167.

Zager RA, Johnson ACM, Becker K. 2011. Acute unilateral ischemic renal injury induces progressive renal inflammation, lipid accumulation, histone modification, and "end-stage" kidney disease. *American Journal of Physiology: Renal Physiology*, **301**(6): F1334–F1345.

Zhang C, Li CL, Xu KX, et al. 2022. The Hippo pathway and its correlation with acute kidney injury. *Zooogical Research*, **43**(5): 897–910.

Zhang J, Wang XM, Wei J, et al. 2020. A two-stage bilateral ischemia-reperfusion injury-induced AKI to CKD transition model in mice. *American Journal of Physiology: Renal Physiology*, **319**(2): F304–F311.

Zhao HJ, Wang SW, Cheng HF, et al. 2006. Endothelial nitric oxide synthase deficiency produces accelerated nephropathy in diabetic mice. *Journal of the American Society of Nephrology*, **17**(10): 2664–2669.

Zhou L, Yu P, Wang TT, et al. 2022. Polydatin attenuates cisplatin-induced acute kidney injury by inhibiting ferroptosis. *Oxidative Medicine and Cellular Longevity*, **2022**(1): 9947191.